
Wukong: 100 Million Large-scale Chinese Cross-modal Pre-training Dataset and A Foundation Framework

Jiaxi Gu^{1*}, Xiaojun Meng^{1*}, Guansong Lu¹, Lu Hou¹, Minzhe Niu¹, Xiaodan Liang^{2†},
Lewei Yao¹, Runhui Huang², Wei Zhang¹, Xin Jiang¹, Chunjing Xu¹, Hang Xu^{1†}

Abstract

Vision-Language Pre-training (VLP) models have shown remarkable performance on various downstream tasks. Their success heavily relies on the scale of pre-trained cross-modal datasets. However, the lack of large-scale datasets and benchmarks in Chinese hinders the development of Chinese VLP models and broader multilingual applications. In this work, we release a large-scale Chinese cross-modal dataset named Wukong, containing 100 million Chinese image-text pairs from the web. Wukong aims to benchmark different multi-modal pre-training methods to facilitate the VLP research and community development. Furthermore, we release a group of models pre-trained with various image encoders (ViT-B/ViT-L/SwinT) and also apply advanced pre-training techniques into VLP such as locked-image text tuning, token-wise similarity in contrastive learning, and reduced-token interaction. Extensive experiments and a deep benchmarking of different downstream tasks are also provided. Experiments show that Wukong can serve as a promising Chinese pre-training dataset and benchmark for different cross-modal learning methods. For the zero-shot image classification task on 10 datasets, Wukong_{ViT-L} achieves an average accuracy of 73.03%. For the image-text retrieval task, Wukong_{ViT-L} achieves a mean recall of 71.6% on AIC-ICC which is 12.9% higher than the result of WenLan 2.0. More information can refer to <https://wukong-dataset.github.io/wukong-dataset/>.

1 Introduction

Pre-training large-scale models on big data, and fine-tuning on downstream tasks, have become an emerging paradigm of artificial intelligence systems. Models such as BERT (Devlin et al., 2019) and GPT (Brown et al., 2020) grow in popularity in the natural language processing community as they possess high transferability to a wide range of downstream tasks or even zero-shot tasks, yielding state-of-the-art performance. Recent works such as CLIP (Radford et al., 2021), ALIGN (Jia et al., 2021) and FILIP (Yao et al., 2022) further extend this diagram to the joint Vision Language Pre-training (VLP) domain and show superior results over state-of-the-art methods on various downstream tasks. This promising direction draws significant attention from both industry and researchers to consider it as the path to the next-generation AI models.

There are two reasons that lead to the success of VLP models. On the one hand, more advanced model architectures such as ViT (Dosovitskiy et al., 2020)/BERT (Devlin et al., 2019) and training objectives like contrastive learning (He et al., 2020), are usually able to lift the powerful generalization and robustness capabilities of learned representations. On the other hand, thanks to the concurrent

¹ Huawei Noah’s Ark Lab * These two authors contribute equally.

² Sun Yat-sen University

† Corresponding authors: xu.hang@huawei.com & xdliang328@gmail.com

Table 1: An overview of datasets for VLP model pre-training.

Dataset	Language	Availability	Image-text pairs
Flickr30k (Young et al., 2014)	English	✓	31,783
CxC (Parekh et al., 2020)	English	✓	247,315
SBU Captions (Ordonez et al., 2011b)	English	✓	1,000,000
Product1M (Zhan et al., 2021)	Chinese	✓	1,000,000
CC12M (Changpinyo et al., 2021)	English	✓	12,000,000
RedCaps (Desai et al., 2021)	English	✓	12,011,111
YFCC100M (Thomee et al., 2016)	English	✓	99,200,000
WIT (Srinivasan et al., 2021)	multilingual	✓	11,500,000
LAION-400M (Schuhmann et al., 2021)	English	✓	400,000,000
JFT-300M (Sun et al., 2017)	English	✗	300,000,000
JFT-3B (Zhai et al., 2021a)	English	✗	3,000,000,000
IG-3.5B-17k (Mahajan et al., 2018)	English	✗	3,500,000,000
M6-Corpus (Lin et al., 2021)	Chinese	✗	60,500,000
Wukong (Ours)	Chinese	✓	101,483,885

advancement in hardware (Stuart and Owens, 2011; Kindratenko et al., 2009) and distributed training frameworks (Narayanan et al., 2021; Rajbhandari et al., 2020; Rasley et al., 2020), more and more data can be fed into a large-scale model to improve the generalization, transferability and zero-shot capability. In either vision or language tasks, pre-training on larger-scale data such as JFT-300M (Sun et al., 2017) in image classification (Riquelme et al., 2021), C4 dataset in T5 (Raffel et al., 2020), has been proven useful and critical for improving downstream task performance via transfer or prompt learning. In addition, recent work (Jia et al., 2021) has already shown the potential of scaling up the VLP model by more than 100 million noisy image-text pairs from the web.

Therefore, the success of VLP models pre-trained on large-scale data urges people to continuously crawl and collect larger image-text dataset. Table 1 shows an overview of many popular datasets in the VLP domain. Publicly-available vision-language English datasets such as Flickr30k (Plummer et al., 2015), SBU Captions (Ordonez et al., 2011a) and CC12M (Sharma et al., 2018) are relatively small at a scale of around 10 million samples, and a larger-scale one is LAION-400M (Schuhmann et al., 2021). However, directly using English datasets to train a model will lead to a great performance drop in translated Chinese downstream tasks. There are a lot of certain Chinese idioms and slang that translated English cannot cover, where machine translation often brings errors that harm the task performance. The current community lacks a large-scale publicly available dataset in Chinese, resulting in (a) the development of the community is stunted; (b) each work uses a secret large dataset to achieve surprisingly good performance that other works cannot fairly compare.

To bridge this gap, we release a large-scale Chinese cross-modal dataset named Wukong, containing 100 million image-text pairs from the web. To guarantee diversity and generalization, our Wukong dataset is collected according to a high-frequency Chinese word list of 200K queries. We also adopt image-based and text-based filtering strategies to further refine it. The resulting dataset is currently the largest Chinese vision-language dataset so far. We perform an analysis of this dataset and show that it covers a wide range of visual and textual concepts.

Training a large-scale VLP model is super expensive. For example, The largest CLIP (Radford et al., 2021) model takes 18 days to train on 592 V100 GPUs, and M6-10T (Lin et al., 2021) is trained on 512 NVIDIA-V100 GPUs for around 10 days. Thus, it is almost impossible for everyone to pre-train a large-scale model due to substantial financial costs and hardware requirements. It is in great demand for researchers to download and reuse various kinds of pre-trained large-scale VLP models. However, the choices of publicly-available large VLP models are also very limited, which hinders the development on downstream tasks of the large-scale model.

In order to contribute to our community, we further release a group of large-scale models pre-trained using different architectures (ResNet (He et al., 2016)/ViT (Dosovitskiy et al., 2020)/SwinT (Liu et al., 2021)) and different methods (CLIP (Radford et al., 2021), FILIP (Yao et al., 2022), and LiT (Zhai et al., 2021b)). As shown in Figure 1, we follow the popular dual-encoder architecture for vision-language representation learning, with the contrastive learning objective. We also provide

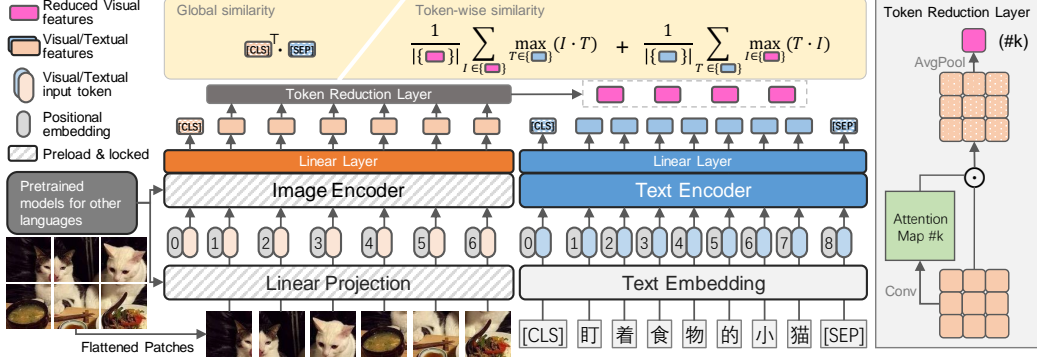


Figure 1: The base model consists of an image encoder and a text encoder with visual tokens and textual tokens as inputs. The input tokens from the two modalities are then concatenated and are added with position embeddings indicating token positions. For the image encoder, weights from an external model trained on datasets of other language are preloaded and locked. We compute the global similarity and token-wise similarity in the contrastive pre-training loss.

an extensive benchmarking of the released models on various downstream tasks, such as zero-shot image classification and Img2Text/Text2Img retrieval. Interesting observations can be found from the results: Firstly, by transferring the image encoder trained on English dataset, we find that it can still work well with Chinese texts for cross-modal pre-training and achieve a good performance on Chinese downstream tasks. Secondly, we find that cross-modal token-wise similarity from FILIP complements various patch-based visual encoders like SwinT and can contribute to better visual and textual representations. More findings can be found in Section 5.

Experiments show that Wukong can serve as a promising Chinese pre-training dataset for different cross-modal learning methods. The pre-trained models show prominent performance on various downstream tasks such as zero-shot image classification and image-text retrieval. Specifically, for zero-shot image classification, our model reaches up to 61.5% average top-1 accuracy on 17 datasets. For the retrieval task, our best model significantly outperforms WenLan 2.0 on AIC-ICC by 10% of top-1 recall for image-to-text retrieval, and 11.6% of top-1 recall for text-to-image retrieval respectively. Visualization on word-patch alignment also shows that our model learns meaningful finer-grained features via the token-wise similarity.

In summary, our main contributions are:

- A public larger-scale Chinese vision and language pre-training dataset with 100 million image-text pairs is released, covering a more comprehensive range of concepts.
- We release a group of large-scale VLP models pre-trained with various popular architectures and methods. An extensive benchmarking of the released models is also provided.
- Our pre-trained model shows state-of-the-art performance on Chinese benchmarks such as zero-shot image classification tasks consisting of seventeen datasets and image-text retrieval tasks consisting of five datasets.

2 Related Work

Vision-Language Pre-training (VLP) Models. There are two typical architectures of VLP models according to the modality interaction methods, i.e., single-stream and dual-stream. Single-stream models (Kim et al., 2021; Li et al., 2019a) directly concatenate the visual and textual embeddings together and feed them to a single transformer-based model. This kind of model can be easily fit into text/image generation tasks to perform image captioning or text-to-image generation, which are usually hard to evaluate and benchmark. Dual-stream models such as ViLBERT (Lu et al., 2019), CLIP (Radford et al., 2021) and ALIGN (Jia et al., 2021) have separate models for each modality. This paradigm is more flexible and efficient when modeling each modality, e.g., CNN for images, Transformers for texts. Moreover, dual-stream models have the merit of efficient inference for downstream tasks such as image-text retrieval, since they can decouple and offline store pre-computed image/text features from encoders. In CLIP (Radford et al., 2021), the authors also evaluate the



Figure 2: Examples of image-text pairs in our Wukong dataset. A diverse range of concepts are included.

image encoder as a self-supervised pre-trained model and show promising results. This paper mainly follows and benchmarks the dual-stream approaches.

Vision-Language Datasets. The current success of VLP models greatly lies in the scale of pre-trained datasets. The publicly-available pre-training datasets used by recent VLP models are mainly image caption data or image-text pair data. Many small-sized datasets (e.g., a few hundred thousand) such as COCO-Captions (Lin et al., 2014), Flickr30k (Plummer et al., 2015), Visual Genome (Krishna et al., 2016), and VQA2 (Goyal et al., 2017) are hand-annotated data that have very limited domain and diversity. On the other hand, pre-training models on online collected data (such as alt-texts from the HTML pages) have shown promising results. CC3M (Sharma et al., 2018), CC12M (Changpinyo et al., 2021) and YFCC100M (Thomee et al., 2016) have millions of image-text pairs in English generated by an online data collection pipeline including image and text filters, as well as text transformations. VLP models on these datasets have shown to be effective in multiple downstream tasks. Moreover, larger-scale datasets with more than 100M samples (e.g., CLIP (Radford et al., 2021); 400M and ALIGN (Jia et al., 2021)): 1.8B) have even armed the recent VLP models with surprisingly good zero-shot recognition ability, but they are not publicly available. Thus, the current community lacks a large-scale Vision-Language dataset in Chinese. We aim to contribute a benchmark Chinese dataset to test various VLP methods on different downstream tasks.

3 Dataset Collection

In this work, we construct a new dataset called Wukong of 100 million image-text pairs collected from the Internet. To cover diverse visual concepts, Wukong dataset is collected according to a list of 200K queries. This base query list is taken from (Song et al., 2018) and then filtered according to the frequency of Chinese words and phrases. After the query list is constructed, we send each query to Baidu Image Search Engine, to get a list of image URLs and corresponding caption information. To keep a balance between different queries, we search for at most 1000 samples per query. Images are then downloaded with previously-obtained image URLs. In this way, we collect a total of 166 million raw \langle image, text \rangle pairs. Then following common practices (Sharma et al., 2018; Changpinyo et al., 2021; Jia et al., 2021), we apply a series of filtering strategies described in the below section to construct the final Wukong dataset. Figure 2 shows some samples within our dataset. In addition, we



Figure 3: The word cloud generated with texts in Wukong dataset. For example, “月” means *month*; “日” is *day*; “做” is *do* and “一个” means *one*.

also build a test set named Wukong50K with 50K samples, which serves as a benchmarking dataset for future models.

3.1 Image-based Filtering

We first filter the data according to the size and aspect ratio of the image. Only images with both dimensions greater than 200 pixels, and the ratio of large-to-small dimensions is no more than 3 are kept. In this way, we filter out images that are too small, or are very tall or wide, which can be of low-resolution after image augmentations like upsampling and square cropping used during pre-training (Yao et al., 2022).

3.2 Text-based Filtering

Secondly, to select samples with high-quality Chinese descriptions of the corresponding image, we filter the data according to the language, length and frequency of the text accompanying an image. Specifically, we first check the language and length. We keep sentences that contain at least one but fewer than 32 Chinese words. We also discard meaningless image descriptions like “000.jpg” from the text. Afterward, texts paired with too many images are usually irrelevant to the content of the images, like “查看源网页” (*View source page*), “展开全文” (*Expand text*), “摄影部落” (*Photography community*). In practice, we set this threshold as 10, i.e., we discard the image-text pairs whose text appears more than 10 times in the whole corpus collected. To protect the privacy of the individuals appearing in the text, we substitute person names with a special token “*人名*” (*Person name*). Besides, we also construct a list of Chinese sensitive words, and image-text pairs containing sensitive words are also discarded.

After applying the above filtering strategies, we finally get a dataset of about 100 million (image, text) pairs. Table 2 shows statistics of our dataset. There are 20,442 unique tokens within the texts of our dataset, and the average number of tokens in each caption is 22. Additionally, in Figure 3, we visualize the distribution of words (consisting of one or more tokens) in our dataset. We use the Chinese text segmentation module *jieba*¹ to generate words and build this word cloud of our dataset.

Table 2: Statistics of Wukong dataset.

Image-text Pairs	Unique Tokens	Tokens per Caption		
		mean	std	median
101,483,885	20,442	22	7	24

¹<https://github.com/fxsjy/jieba>

4 Methodology

4.1 Text-Image Joint Alignment

Following the recent well-proven methods (Radford et al., 2021; Yao et al., 2022), we adopt the contrastive pre-training architecture as shown in Figure 1. We use a dual-stream model with Transformer-based text and image encoders. These two encoders convert textual and visual input tokens to embeddings of the same dimension. In this learned joint embedding space, we use a contrastive loss to encourage the paired image and text to have similar embeddings, while non-paired ones to have distinct embeddings. In (Radford et al., 2021) and (Jia et al., 2021), this cross-modal similarity is computed via dot product between the global features of the entire image and that of the text sequence. On the other hand, in (Yao et al., 2022), the similarity is computed based on a finer-grained interaction between the image patches and textual tokens, which also brings surprisingly good word-patch alignment and learns meaningful fine-grained features with promising localization ability.

4.2 Model Architectures

Visual Encoder. Two types of visual encoders, *i.e.*, Vision Transformer (Dosovitskiy et al., 2020) (ViT) and Swin Transformer (Liu et al., 2021) (SwinT), are used as backbones for training different model variants. For ViT, the input image is first rescaled into a standard size and then split into fixed-size patches. Each of the patches is linearly embedded via a trainable linear projection. The resulting sequence of patch vectors is fed to a standard transformer encoder. Different from ViT, SwinT uses a hierarchical transformer that computes representation with shifted windows, which limits the original self-attention computation to non-overlapping local windows while also allowing for cross-window connection.

Textual Encoder. The textual encoder is a standard decoder-only transformer as in (Radford et al., 2021). We use WordPiece (Wu et al., 2016) with a vocabulary size of 21,128 for Chinese text tokenization. Similar to (Pires et al., 2019), we add spaces around Chinese characters before applying WordPiece so that Chinese is effectively character-tokenized. We add two special tokens (*i.e.*, [CLS] and [SEP]) at the beginning and ending of each text sequence. The text encoder has 12 layers, each of which has 12 attention heads and a hidden state dimension of 768.

Linear Projection of the Encoders. On the top of the visual and textual encoders, the global representations of visual token sequence (*e.g.*, [CLS] token for ViT; average pooled representation of all patch tokens for Swin Transformer) and textual token sequence (*e.g.*, textual [SEP] token) are linearly projected to the common multi-modalities space, followed by L2-normalization separately.

Token Reduction Layer. Instead of only computing the cross-modal similarity between global representations of sequences, we experiment with a late interaction method as introduced in FILIP (Yao et al., 2022). We aim to take into account the fine-grained token-wise interaction between image patches and text tokens. It could potentially mine more detailed semantic word-patch alignment between two modalities. Meanwhile, as a large amount of computation is introduced by this token-wise interaction, we propose a token reduction layer inspired by (Ryoo et al., 2021). It aims to learn a small set of tokens (*e.g.*, 12 or 24) from the whole output tokens of visual encoder (*e.g.*, 16×16 in ViT-L/14), and use them for the reduced-token interaction as described in Section 4.4. The token reduction layer can largely reduce the computation cost for the late interaction method.

4.3 Pre-training Objectives

Cross-modal contrastive learning is one effective approach for training models from paired image-text data, which can learn representations of two modalities simultaneously by distinguishing the paired and unpaired samples. We use \mathcal{I} to denote the set of image samples while \mathcal{T} is for text data. Given an image sample $\mathbf{x}^I \in \mathcal{I}$ and a text sample $\mathbf{x}^T \in \mathcal{T}$, the training objective is to make the learned image and text representations in the joint multi-modal space be close if they are paired while far apart otherwise. For a training batch consisting of b image-text pairs $\{\mathbf{x}_k^I, \mathbf{x}_k^T\}_{k=1}^b$, \mathbf{x}_k^T (*resp.* \mathbf{x}_k^I) is positive to \mathbf{x}_k^I (*resp.* \mathbf{x}_k^T) while negative to all other texts (*resp.* images) in the same batch. Therefore,

the image-to-text and text-to-image contrastive losses for $(\mathbf{x}_k^I, \mathbf{x}_k^T)$ can be formulated as:

$$\mathcal{L}_k^I(\mathbf{x}_k^I, \{\mathbf{x}_j^T\}_{j=1}^b) = -\frac{1}{b} \log \frac{\exp(s_{k,k}^I)}{\sum_{j=1}^b \exp(s_{k,j}^I)}, \quad (1)$$

$$\mathcal{L}_k^T(\mathbf{x}_k^T, \{\mathbf{x}_j^I\}_{j=1}^b) = -\frac{1}{b} \log \frac{\exp(s_{k,k}^T)}{\sum_{j=1}^b \exp(s_{k,j}^T)}, \quad (2)$$

where $s_{k,j}^I$ denotes the similarity of the k -th image to the j -th text, while $s_{k,j}^T$ denotes the similarity between the k -th text to the j -th image. The total loss \mathcal{L} of this training batch is then computed as:

$$\mathcal{L} = \frac{1}{2} \sum_{k=1}^b (\mathcal{L}_k^I + \mathcal{L}_k^T). \quad (3)$$

In this work, we explore two typical ways of measuring the similarity between an image and a text. The learned representations of the image and text are denoted by $\mathbf{z}^I \in \mathbb{R}^{n_1 \times d}$ and $\mathbf{z}^T \in \mathbb{R}^{n_2 \times d}$, respectively. Here n_1 and n_2 are the number of (non-padded) tokens in each image and text.

Global Similarity. In CLIP (Radford et al., 2021) and ALIGN (Jia et al., 2021), the similarity is computed via dot product of the global features of the entire image and text sequence. Specifically, the global similarity between the image and text is computed as

$$s_{i,j}^I = s_{i,j}^T = [\mathbf{z}_i^I]_{\text{CLS}}^\top [\mathbf{z}_j^T]_{\text{SEP}}, \quad (4)$$

where $[\mathbf{z}_i^I]_{\text{CLS}}$ denotes the feature vector of the [CLS] token of the i -th image and $[\mathbf{z}_j^T]_{\text{SEP}}$ denotes the feature vector of the [SEP] token of the j -th text. Since Swin Transformer has no [CLS] token, we use the average pooling on the features of all patch tokens to represent it.

Token-wise Similarity. In FILIP (Yao et al., 2022), the similarity is computed based on a finer-grained interaction between the image patches and textual tokens, which also brings surprisingly good alignment and learns meaningful fine-grained features with promising localization ability. For i -th image, each visual token $[\mathbf{z}_i^I]_k$ in it computes a similarity with all non-padded textual tokens of the j -th text. Then the maximum one is used to represent the token-wise similarity between this visual token and the j -th text. Finally, we regard the average token-wise maximum similarity of all non-padded tokens in this i -th image as the cross-modal similarity

$$s_{i,j}^I = \frac{1}{n_1} \sum_{k=1}^{n_1} [\mathbf{z}_i^I]_k^\top [\mathbf{z}_j^T]_{m_k^I}, \quad (5)$$

where $m_k^I = \arg \max_{0 \leq r < n_2} [\mathbf{z}_i^I]_k^\top [\mathbf{z}_j^T]_r$. The similarity of a text to an image can be computed in the same way, except that we exclude the [CLS], [SEP] and all padding tokens as in FILIP (Yao et al., 2022).

4.4 Reduced-token Interaction

Obviously, using the token-wise similarity introduces a larger amount of computation. The computation cost of it is about $2 \times n_1 \times n_2$ times than that of global similarity as shown in Equation 4 and Equation 5. The number of visual tokens n_1 is normally predefined while the number of textual tokens n_2 depends on the text input. To reduce the computation cost of full token-wise similarity, an efficient way is to decrease the number of tokens involved in similarity calculation and we call this reduced-token interaction. For this purpose, we propose a learnable token reduction layer on top of visual features output by the image encoder. The workflow of this layer is described in the right part of Figure 1.

Since the number of visual tokens is usually much larger than that of textual tokens, visual tokens are more necessary to be decreased. Denoting the visual tokens of an image sample as $\mathbf{z}^I \in \mathbb{R}^{n_1 \times d}$, we aim to get a new $Z^I = f(\mathbf{z}^I) \in \mathbb{R}^{n' \times d}$ in which f denotes the function of token reduction and n' denotes the reduced token number. Finally, \mathbf{z}^I is replaced by Z^I in Equation 5 to calculate the token-wise similarity. In general, given the output number of tokens n' , the k -th visual token $Z_k^I \in \mathbb{R}^d$ can be formulated by:

$$Z_k^I = \text{AvgPool}(\text{Conv}_k(\mathbf{z}^I) \odot \mathbf{z}^I), \quad k \in \{1, 2, \dots, n'\} \quad (6)$$

where \odot represents Hadamard product. Firstly, $z_k^I \in \mathbb{R}^{n_1 \times d}$ is reshaped to $z_k^I \in \mathbb{R}^{H \times W \times d}$ in which H and W respectively represents the vertical and horizontal numbers of visual tokens. Then, the k -th attention map is computed via $Conv_k : \mathbb{R}^{H \times W \times d} \rightarrow \mathbb{R}^{H \times W \times 1}$ which is implemented using two convolutional layers. We share the weight of $Conv_k$ across all k tokens. Finally, a spatial global average pooling $AvgPool : \mathbb{R}^{H \times W \times d} \rightarrow \mathbb{R}^d$ is used to get the final k -th visual token.

4.5 Locked-image Text Tuning

Inspired by ‘‘Locked-image Text tuning’’ (LiT-tuning) (Zhai et al., 2021b) which shows that a locked pre-trained image encoder with unlocked text encoder works well, we take advantage of pre-trained image encoders for contrastive learning. In particular, this setting aims to teach a Chinese text encoder to read out suitable representations from an existing image encoder pre-trained on English datasets. techniques for learning image descriptors and vision-language alignment (Zhai et al., 2021b). And the image descriptors are beforehand well pre-trained using relatively clean or (semi-) manually labeled images. In this work, we extend this idea to multilingual data sources, and try to align a locked image encoder pre-trained on English data sources and a trainable Chinese text encoder. Moreover, the LiT-tuning method significantly speeds up the training process and reduces memory requirements since no gradients need to be computed for the visual encoder. Empirical results in Section 5 confirm the effectiveness of our method.

5 Experiments

5.1 Experimental Setup

Model Architectures. Following the existing VLP models, *e.g.*, CLIP (Radford et al., 2021), ALIGN (Jia et al., 2021), we employ a dual-encoder architecture as illustrated in Figure 1. As only text-encoder tuning shows good performance (Zhai et al., 2021b), our visual encoder is initialized and locked with pre-trained models, *e.g.*, ViT-B, ViT-L from CLIP², Swin-L from Swin Transformer³, and only the text encoder is trained. According to the different types of visual encoders, we train three model variants, *i.e.*, Wukong_{ViT-B}, Wukong_{ViT-L} and Wukong_{Swin}, using the token-wise similarity with our proposed reduced-token interaction. Detailed settings are described in Table 3.

Model Training Settings. For better generalization and data-efficiency, we employ Autoaugment (Cubuk et al., 2019) for image data augmentation that aims to build more image-text pairs. All of our models are trained using Nvidia V100 GPUs and Ascend cards. Specifically, Wukong_{ViT-B} is trained using 32 GPUs for 3 days, Wukong_{ViT-L} is trained using 32 GPUs for 10 days and Wukong_{Swin} is trained using 40 GPUs for 5 days. In the training, we use the LAMB optimizer (You et al., 2020) and the cosine learning rate schedule with a linear warmup (Loshchilov and Hutter, 2016). Weight decay regularization is applied to all parameters except for bias, layer normalization, token embedding, positional embedding and temperature in the contrastive loss. The detailed hyperparameters are shown in Table 4. In order to pick the optimal checkpoint out, ImageNet dataset (Deng et al., 2009) with translated label names is used for zero-shot validation.

Table 3: Detailed settings of our model variants. The input image resolution is 224×224 and text context length is 32. For the text encoder, 12 layers of Transformers with a width of 768 and 12 heads are used.

Model	Embedding dimension	Image encoder	Token Reduction
Wukong _{ViT-B}	512	ViT-B/32	12
Wukong _{ViT-L}	768	ViT-L/14	24
Wukong _{Swin}	768	Swin-L	12

Table 4: Hyper-parameters for training.

Initial Temp.	LAMB			Total Epochs
	β_1	β_2	ϵ	
0.07	0.9	0.999	10^{-2}	20

²<https://github.com/openai/CLIP/>

³<https://github.com/microsoft/Swin-Transformer>

Table 5: Top-1 accuracy (%) of zero-shot image classification. All the model variants are trained using 100-million Wukong dataset with token-wise similarity and reduced-token interaction method except for those marked with special superscripts. The superscript “F” means models are trained using Full-token token-wise similarity and “G” means using Global similarity. Results in **bold** means the best within a same image encoder and those underline represents the best among all methods.

Model \ Dataset	CIFAR10	CIFAR100	Caltech101	Caltech256	DTD	Sports	Flowers	SUN397	EuroSAT	ImageNet	Average
Wukong ^G _{VIT-B}	89.4	62.5	89.2	82.7	36.2	93.1	52.6	55.8	25.7	47.7	63.49
Wukong ^F _{VIT-B}	87.0	53.3	83.1	71.0	28.9	91.2	48.8	50.0	29.5	38.1	58.09
Wukong _{VIT-B}	87.1	62.6	89.1	82.3	37.3	95.6	64.8	56.0	32.6	49.1	65.65
Wukong ^G _{VIT-L}	94.1	71.3	91.9	89.0	45.4	98.7	72.3	62.6	42.8	57.9	72.60
Wukong ^F _{VIT-L}	90.6	66.3	89.9	86.2	46.4	97.8	69.4	60.2	25.5	54.0	68.63
Wukong _{VIT-L}	95.4	77.1	92.4	89.2	40.9	99.1	68.9	62.0	50.3	55.0	73.03
Wukong ^G _{Swin}	94.8	75.8	90.7	88.3	40.0	97.5	71.0	57.3	22.3	58.0	69.57
Wukong ^F _{Swin}	95.5	77.2	91.6	88.4	39.8	99.1	75.1	56.5	21.0	58.5	70.27
Wukong _{Swin}	<u>95.3</u>	<u>76.8</u>	89.8	87.1	33.7	97.8	76.9	56.3	19.3	58.2	69.12

5.2 Zero-shot Image Classification

We evaluate our pre-trained models for zero-shot classification task on 10 datasets whose class labels are translated from English. To make the evaluation results more reliable, the translation process is done with an online machine translation service followed by a manual refinement. We publish the annotated Chinese versions of these datasets for future evaluation in the research community in <https://wukong-dataset.github.io/wukong-dataset/>.

Prompt Ensemble. Text prompts are often used as a class label augmentation to get a better performance in zero-shot image classification task (Radford et al., 2021; Yao et al., 2022). For simplicity, instead of designing prompts manually, we use fixed 80 text prompts which are used on ImageNet dataset by CLIP. Since the original prompts are in English, they are manually translated into Chinese. It is possible that adding extra descriptions as a part of text prompts specific to each dataset may further improve the results. Since our paper aims to provide a benchmark dataset with pre-trained models, we stick to the general-purpose prompt templates, and leave the design of better prompt templates for each task as a future work. Note that when using the global similarity, we follow CLIP to ensemble different prompt templates by using their mean textual representation, i.e., we sum different templates for the same class label to form a mean textual representation. While for the token-wise similarity, since there is no global representation, we simply ensemble prompt templates by their mean token-wise similarity to images.

The evaluation of zero-shot image classification on different datasets is illustrated in Table 5. For our proposed models, i.e., Wukong_{VIT-B}, Wukong_{VIT-L} and Wukong_{Swin}, we also evaluate multiple model variants with global similarity (marked with “G”) or full token-wise interaction (marked with “F”). Among all the model variants, Wukong_{VIT-L} obtains the best result of 73.03%. We find that using token-wise similarity together with reduced-token interaction brings significant improvement especially for VIT-based models. Take Wukong_{VIT-B} as an example, using the token reduction layer achieves the highest accuracy 65.65% among all. However, the token reduction layer in SwinT is less effective. The reason might be that patch merging in SwinT has already served a similar purpose on selecting and merging the important visual patch tokens.

In summary, the zero-shot classification performances on various tasks show the effectiveness of our dataset and models. Although these visual encoders are all pre-trained on English datasets, e.g., ImageNet-22K and YFCC100M (Thomee et al., 2016), we find that the image feature computed by them is still reliable and expressive for efficiently pairing Chinese texts and images in our dataset.

Table 6: Results of zero-shot image-text retrieval on different datasets. MR (Mean Recall) denotes the average of Recall@K with $K \in \{1, 5, 10\}$. Results in **bold** mean the best.

Dataset	Method	Image-to-Text Retrieval			Text-to-Image Retrieval			MR
		R@1	R@5	R@10	R@1	R@5	R@10	
Flickr8K-CN	Wukong _{ViT-B}	55.4	82.3	90.0	43.2	71.3	81.3	70.6
	Wukong _{ViT-L}	61.4	86.2	93.6	46.0	74.5	84.5	74.4
	Wukong _{Swin}	47.2	78.8	87.6	36.6	64.8	76.2	65.2
Flickr30K-CN	Wukong _{ViT-B}	66.2	88.7	94.3	45.7	73.8	82.2	75.1
	Wukong _{ViT-L}	76.1	94.8	97.5	51.7	78.9	86.3	80.9
	Wukong _{Swin}	58.7	86.7	92.7	40.9	68.0	78.4	70.9
COCO-CN	Wukong _{ViT-B}	48.3	77.8	88.8	49.2	79.4	87.9	71.9
	Wukong _{ViT-L}	55.2	81.0	90.6	53.4	80.2	90.1	75.1
	Wukong _{Swin}	47.3	78.0	88.3	46.4	77.0	87.6	70.8
MUGE	Wukong _{ViT-B}	-	-	-	33.4	59.3	69.7	54.1
	Wukong _{ViT-L}	-	-	-	42.7	69.0	78.0	63.2
	Wukong _{Swin}	-	-	-	34.5	60.6	71.2	55.5

5.3 Image-Text Retrieval

In this section, we evaluate our models on two sub-tasks, including image-to-text retrieval and text-to-image retrieval. In the image-to-text retrieval, the model retrieves a target text from a set of candidates given an image as query, or vice versa for the text-to-image retrieval. We benchmark our models on 6 different datasets, including Flickr8K-CN (Li et al., 2016), Flickr30K-CN (Lan et al., 2017), COCO-CN (Li et al., 2019b), AIC-ICC (Wu et al., 2017), MUGE⁴ and Wukong50K.

For each dataset, our pre-trained models are evaluated in both zero-shot and fine-tuned settings. Following common practices, we report Recall@K (recall of top K candidates) with $K = 1, 5, 10$ for both image-to-text and text-to-image retrieval on all datasets except for MUGE, which only has the text-to-image retrieval setting. The average of Recall@K, i.e., Mean Recall (MR), is used for the final comparison. We report results on the test sets, except for MUGE and AIC-ICC where test sets are not released. For MUGE, we report results on the validation set, and for AIC-ICC, following the setting of WenLan 2.0 (Fei et al., 2021), we take the first 10K images along with their corresponding 50K pieces of texts from the validation set for testing.

Table 6 and Table 7 show the results of zero-shot and fine-tuned image-text retrieval respectively. Our Wukong_{ViT-L} achieves the best results among different model variations and datasets, in either zero-shot or fine-tuned setting. Compared with baseline methods, on AIC-ICC, Wukong significantly outperforms WenLan 2.0 by around 12.9%, which was pre-trained on a larger dataset consisting of 650 million image-text pairs. For the COCO-CN dataset, our Wukong models also achieve comparable performance to state-of-the-art methods. Overall, experimental results demonstrate the capabilities of our pre-trained models.

5.4 Visualization of word-patch alignment

Since we follow the fine-grained interaction in FILIP (Yao et al., 2022), our models Wukong_{ViT-L} and Wukong_{Swin} likewise own the capability of capturing the correspondence between images and Chinese texts. Note that they are trained using the token-wise similarity. We exclude ones with the global similarity since they lack of word-patch alignment capability, which has also been evidenced in previous work (Yao et al., 2022).

As shown in Figure 4, we visualize images from six labels in the Chinese ImageNet. We apply the same visualization method from FILIP (Yao et al., 2022), to align textual tokens and image patch tokens. In particular, we calculate the token-wise similarity between each image patch token and all tokenized textual tokens from the text label, i.e., [CLS] {class label tokens} [SEP], as illustrated in the Section 4.3. For each image patch, the position index of textual tokens with the maximum

⁴<https://tianchi.aliyun.com/muge>

Table 7: Results of fine-tuned image-text retrieval on different datasets. Those in **bold** means the best among different Wukong variants and those with underline means the best among all methods.

Dataset	Method	Image-to-Text Retrieval			Text-to-Image Retrieval			MR
		R@1	R@5	R@10	R@1	R@5	R@10	
Flickr8K-CN	Wukong _{ViT-B}	71.7	91.5	96.6	58.4	85.4	92.0	82.6
	Wukong _{ViT-L}	83.3	97.3	99.5	70.1	91.9	96.4	89.7
	Wukong _{Swin}	74.9	93.6	97.8	57.9	85.1	92.6	83.6
Flickr30K-CN	Wukong _{ViT-B}	83.9	97.6	99.0	67.6	89.6	94.2	88.7
	Wukong _{ViT-L}	92.7	99.1	99.6	77.4	94.5	97.0	93.4
	Wukong _{Swin}	86.2	98.1	99.4	67.4	89.9	94.5	89.3
COCO-CN	EmbN (Wang et al., 2018)	-	-	-	-	-	-	73.2
	PARALLEL-EmbN (Gella et al., 2017)	-	-	-	-	-	-	76.0
	S-LIWE (Wehrmann et al., 2019)	-	-	-	-	-	-	73.6
	M ³ P (Ni et al., 2021)	-	-	-	-	-	-	86.2
	UNITER (Chen et al., 2020)	-	-	-	-	-	-	87.3
	LightningDOT (Sun et al., 2021)	-	-	-	-	-	-	88.4
	UC ² (Zhou et al., 2021)	-	-	-	-	-	-	<u>89.8</u>
	Wukong _{ViT-B}	65.8	90.3	96.6	67.0	91.4	96.7	84.6
	Wukong _{ViT-L}	73.3	94.0	98.0	74.0	94.4	98.1	88.6
	Wukong _{Swin}	67.4	92.4	97.5	66.0	92.6	97.1	85.5
AIC-ICC	WenLan 2.0 (Fei et al., 2021)	45.6	68.0	76.3	34.1	58.9	69.1	58.7
	Wukong _{ViT-B}	47.5	70.6	78.6	36.7	36.7	71.7	57.0
	Wukong _{ViT-L}	61.6	80.5	86.1	48.6	72.5	80.2	71.6
	Wukong _{Swin}	50.9	73.6	81.5	38.6	64.1	73.6	63.7
MUGE	Wukong _{ViT-B}	-	-	-	39.2	66.9	77.4	61.2
	Wukong _{ViT-L}	-	-	-	52.7	77.9	85.6	72.1
	Wukong _{Swin}	-	-	-	43.8	71.9	81.7	65.8
Wukong50k	Wukong _{ViT-B}	83.7	75.5	85.5	39.1	72.5	83.4	73.3
	Wukong _{ViT-L}	59.9	90.4	96.0	55.4	88.1	94.7	80.8
	Wukong _{Swin}	43.5	77.6	87.1	38.5	72.8	83.7	67.2

similarity is considered as its predicted text token. Note that the Chinese class label is often tokenized to more than one token. We highlight all the predicted position indices that correspond to the class label, and place them at the center of the corresponding patches.

From Figure 4, we surprisingly find that both models are able to predict image patches of the target object. For Wukong_{ViT-L} with each image patchified to 16×16 , such word-patch alignment is more fine-grained than Wukong_{Swin} with the output resolution as 7×7 . Take Figure 4 (e) as an example, Wukong_{ViT-L} is even able to align Chinese tokens “教” and “堂”, which means church as one word, to the smaller church in the bottom-right corner. Wukong_{ViT-L} also well outlines the hummingbird in the example of Figure 4 (c), while Wukong_{Swin} often aligns to the main body of the target object. Another interesting observation is that these Chinese pre-trained models are able to align image patches to English tokens as shown in Figure 4 (d). The main reason lies in that the vocabulary used from BERT (Devlin et al., 2019) also includes multilingual words such as “iPod”.

This visualization of word-patch alignment evidences the effectiveness of cross-modal token-wise similarity even in the LiT-tuning setting. Though the visual encoder (i.e., ViT-L/14 or Swin-L) is locked in the pre-training phase, the learnable linear projection layer on top of it, is still able to align patches and words in a fine-grained manner. We also find that this token-wise similarity in loss function works across various patch-based visual encoders, not only the traditional ViT architecture but also SwinT that uses the sophisticated shifted windowing attention and patch merging. Given this promising capability of aligning words and patches, our experiment offers a potential solution towards image object localization.

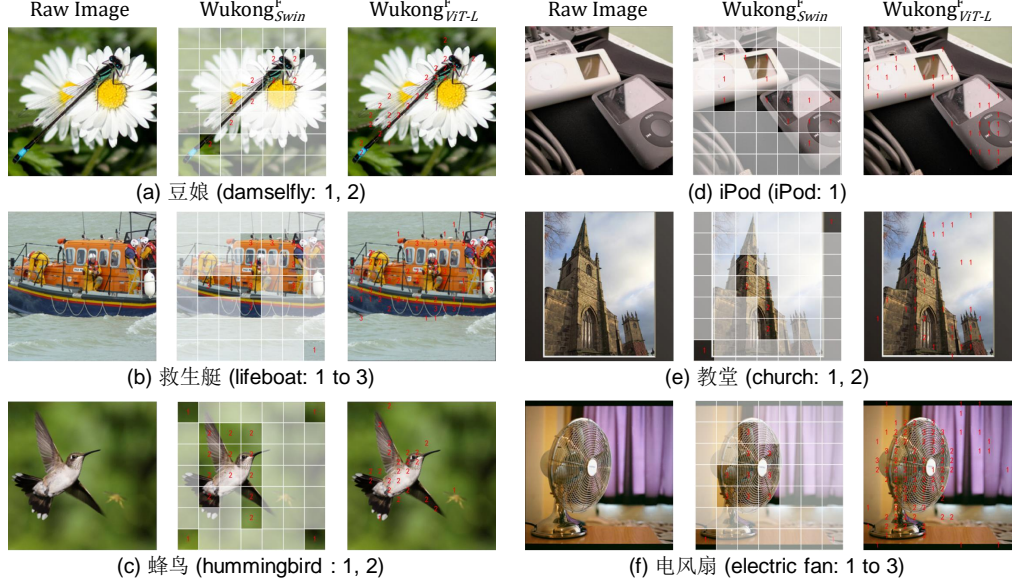


Figure 4: Visualization of word-patch alignment. We randomly choose six classes in the Chinese ImageNet dataset. Each Chinese label name is used as a prompt, whose English text is described in the parentheses. Behind which, the tail numbers indicate the location indices of this class label in the tokenized textual input. Take (a) as an example, the number 0 always represents [CLS], the number 1 is the tokenized “豆” and the number 2 is “娘”. Indices of the tokenized label name are highlighted in red.

6 Conclusion

In this work, we build a large-scale Chinese vision-language dataset called Wukong. To the best of our knowledge, it is the first hundred-million level dataset specific for Chinese language and it paves the way for future research on Chinese cross-modal pre-training. Meanwhile, using this dataset, we propose three Chinese VLP models, i.e., Wukong_{ViT-B}, Wukong_{ViT-L} and Wukong_{Swin}. Experiments evidence that it is possible to apply the frozen visual encoders pre-trained on English dataset to Chinese multi-modal pre-training. It also shows that Wukong can serve as a promising Chinese pre-training dataset and benchmark for different cross-modal learning methods. Our pre-trained Wukong_{ViT-L} achieves state-of-the-art performance on Chinese benchmarks such as zero-shot image classification and image-text retrieval tasks. In the future, we plan to explore more solutions to train multilingual cross-modal models with the Wukong dataset.

References

T. B. Brown, B. Mann, N. Ryder, M. Subbiah, J. Kaplan, P. Dhariwal, A. Neelakantan, P. Shyam, G. Sastry, A. Askell, et al. Language models are few-shot learners. In *Advances in neural information processing systems*, 2020.

S. Changpinyo, P. Sharma, N. Ding, and R. Soricut. Conceptual 12M: Pushing web-scale image-text pre-training to recognize long-tail visual concepts. In *IEEE/CVF Conference on Computer Vision and Pattern Recognition*, 2021.

Y.-C. Chen, L. Li, L. Yu, A. El Kholy, F. Ahmed, Z. Gan, Y. Cheng, and J. Liu. Uniter: Universal image-text representation learning. In *European conference on computer vision*, pages 104–120. Springer, 2020.

E. D. Cubuk, B. Zoph, D. Mane, V. Vasudevan, and Q. V. Le. Autoaugment: Learning augmentation strategies from data. In *Proceedings of the IEEE/CVF Conference on Computer Vision and Pattern Recognition*, pages 113–123, 2019.

J. Deng, W. Dong, R. Socher, L.-J. Li, K. Li, and L. Fei-Fei. Imagenet: A large-scale hierarchical image database. In *2009 IEEE conference on computer vision and pattern recognition*, pages 248–255. Ieee, 2009.

K. Desai, G. Kaul, Z. Aysola, and J. Johnson. Redcaps: Web-curated image-text data created by the people, for the people. *arXiv preprint arXiv:2111.11431*, 2021.

J. Devlin, M.-W. Chang, K. Lee, and K. Toutanova. Bert: Pre-training of deep bidirectional transformers for language understanding. In *Annual Conference of the North American Chapter of the Association for Computational Linguistics*, 2019.

A. Dosovitskiy, L. Beyer, A. Kolesnikov, D. Weissenborn, X. Zhai, T. Unterthiner, M. Dehghani, M. Minderer, G. Heigold, S. Gelly, et al. An image is worth 16x16 words: Transformers for image recognition at scale. In *International Conference on Learning Representations*, 2020.

N. Fei, Z. Lu, Y. Gao, G. Yang, Y. Huo, J. Wen, H. Lu, R. Song, X. Gao, T. Xiang, et al. Wenlan 2.0: Make ai imagine via a multimodal foundation model. *arXiv preprint arXiv:2110.14378*, 2021.

S. Gella, R. Sennrich, F. Keller, and M. Lapata. Image pivoting for learning multilingual multimodal representations. *arXiv preprint arXiv:1707.07601*, 2017.

Y. Goyal, T. Khot, D. Summers-Stay, D. Batra, and D. Parikh. Making the v in vqa matter: Elevating the role of image understanding in visual question answering. In *Proceedings of the IEEE conference on computer vision and pattern recognition*, pages 6904–6913, 2017.

K. He, X. Zhang, S. Ren, and J. Sun. Deep residual learning for image recognition. In *Proceedings of the IEEE conference on computer vision and pattern recognition*, pages 770–778, 2016.

K. He, H. Fan, Y. Wu, S. Xie, and R. Girshick. Momentum contrast for unsupervised visual representation learning. In *Proceedings of the IEEE/CVF conference on computer vision and pattern recognition*, pages 9729–9738, 2020.

C. Jia, Y. Yang, Y. Xia, Y.-T. Chen, Z. Parekh, H. Pham, Q. V. Le, Y. Sung, Z. Li, and T. Duerig. Scaling up visual and vision-language representation learning with noisy text supervision. In *International Conference on Machine Learning*, 2021.

W. Kim, B. Son, and I. Kim. Vilt: Vision-and-language transformer without convolution or region supervision. In *International Conference on Machine Learning*, 2021.

V. V. Kindratenko, J. J. Enos, G. Shi, M. T. Showerman, G. W. Arnold, J. E. Stone, J. C. Phillips, and W.-m. Hwu. Gpu clusters for high-performance computing. In *2009 IEEE International Conference on Cluster Computing and Workshops*, pages 1–8. IEEE, 2009.

R. Krishna, Y. Zhu, O. Groth, J. Johnson, K. Hata, J. Kravitz, S. Chen, Y. Kalantidis, L.-J. Li, D. A. Shamma, et al. Visual genome: Connecting language and vision using crowdsourced dense image annotations. *arXiv preprint arXiv:1602.07332*, 2016.

W. Lan, X. Li, and J. Dong. Fluency-guided cross-lingual image captioning. In *Proceedings of the 25th ACM international conference on Multimedia*, pages 1549–1557, 2017.

L. H. Li, M. Yatskar, D. Yin, C.-J. Hsieh, and K.-W. Chang. Visualbert: A simple and performant baseline for vision and language. *arXiv preprint arXiv:1908.03557*, 2019a.

X. Li, W. Lan, J. Dong, and H. Liu. Adding chinese captions to images. In *Proceedings of the 2016 ACM on international conference on multimedia retrieval*, pages 271–275, 2016.

X. Li, C. Xu, X. Wang, W. Lan, Z. Jia, G. Yang, and J. Xu. Coco-cn for cross-lingual image tagging, captioning, and retrieval. *IEEE Transactions on Multimedia*, 21(9):2347–2360, 2019b.

J. Lin, R. Men, A. Yang, C. Zhou, M. Ding, Y. Zhang, P. Wang, A. Wang, L. Jiang, X. Jia, et al. M6: A chinese multimodal pretrainer. *arXiv preprint arXiv:2103.00823*, 2021.

T.-Y. Lin, M. Maire, S. Belongie, J. Hays, P. Perona, D. Ramanan, P. Dollár, and C. L. Zitnick. Microsoft coco: Common objects in context. In *European conference on computer vision*, pages 740–755. Springer, 2014.

Z. Liu, Y. Lin, Y. Cao, H. Hu, Y. Wei, Z. Zhang, S. Lin, and B. Guo. Swin transformer: Hierarchical vision transformer using shifted windows. In *Proceedings of the IEEE/CVF International Conference on Computer Vision*, pages 10012–10022, 2021.

I. Loshchilov and F. Hutter. Sgdr: Stochastic gradient descent with warm restarts. *arXiv preprint arXiv:1608.03983*, 2016.

J. Lu, D. Batra, D. Parikh, and S. Lee. Vilbert: pretraining task-agnostic visiolinguistic representations for vision-and-language tasks. In *International Conference on Neural Information Processing Systems*, pages 13–23, 2019.

D. Mahajan, R. Girshick, V. Ramanathan, K. He, M. Paluri, Y. Li, A. Bharambe, and L. Van Der Maaten. Exploring the limits of weakly supervised pretraining. In *Proceedings of the European conference on computer vision (ECCV)*, pages 181–196, 2018.

D. Narayanan, M. Shoeybi, J. Casper, P. LeGresley, M. Patwary, V. A. Korthikanti, D. Vainbrand, P. Kashinkunti, J. Bernauer, B. Catanzaro, et al. Efficient large-scale language model training on gpu clusters. *arXiv preprint arXiv:2104.04473*, 2021.

M. Ni, H. Huang, L. Su, E. Cui, T. Bharti, L. Wang, D. Zhang, and N. Duan. M3p: Learning universal representations via multitask multilingual multimodal pre-training. In *Proceedings of the IEEE/CVF Conference on Computer Vision and Pattern Recognition*, pages 3977–3986, 2021.

V. Ordonez, G. Kulkarni, and T. Berg. Im2text: Describing images using 1 million captioned photographs. *Advances in neural information processing systems*, 24, 2011a.

V. Ordonez, G. Kulkarni, and T. Berg. Im2text: Describing images using 1 million captioned photographs. In J. Shawe-Taylor, R. Zemel, P. Bartlett, F. Pereira, and K. Q. Weinberger, editors, *Advances in Neural Information Processing Systems*, volume 24. Curran Associates, Inc., 2011b.

Z. Parekh, J. Baldridge, D. Cer, A. Waters, and Y. Yang. Crisscrossed captions: Extended intramodal and intermodal semantic similarity judgments for ms-coco. *arXiv preprint arXiv:2004.15020*, 2020.

T. Pires, E. Schlinger, and D. Garrette. How multilingual is multilingual bert? *arXiv preprint arXiv:1906.01502*, 2019.

B. A. Plummer, L. Wang, C. M. Cervantes, J. C. Caicedo, J. Hockenmaier, and S. Lazebnik. Flickr30k entities: Collecting region-to-phrase correspondences for richer image-to-sentence models. In *Proceedings of the IEEE international conference on computer vision*, pages 2641–2649, 2015.

A. Radford, J. W. Kim, C. Hallacy, A. Ramesh, G. Goh, S. Agarwal, G. Sastry, A. Askell, P. Mishkin, J. Clark, et al. Learning transferable visual models from natural language supervision. In *International Conference on Machine Learning*, pages 8748–8763. PMLR, 2021.

C. Raffel, N. Shazeer, A. Roberts, K. Lee, S. Narang, M. Matena, Y. Zhou, W. Li, and P. J. Liu. Exploring the limits of transfer learning with a unified text-to-text transformer. *Journal of Machine Learning Research*, 21: 1–67, 2020.

S. Rajbhandari, J. Rasley, O. Ruwase, and Y. He. Zero: Memory optimizations toward training trillion parameter models. In *SC20: International Conference for High Performance Computing, Networking, Storage and Analysis*, pages 1–16. IEEE, 2020.

J. Rasley, S. Rajbhandari, O. Ruwase, and Y. He. Deepspeed: System optimizations enable training deep learning models with over 100 billion parameters. In *Proceedings of the 26th ACM SIGKDD International Conference on Knowledge Discovery & Data Mining*, pages 3505–3506, 2020.

C. Riquelme, J. Puigcerver, B. Mustafa, M. Neumann, R. Jenatton, A. Susano Pinto, D. Keysers, and N. Houlsby. Scaling vision with sparse mixture of experts. *Advances in Neural Information Processing Systems*, 34, 2021.

M. Ryoo, A. Piergiovanni, A. Arnab, M. Dehghani, and A. Angelova. Tokenlearner: Adaptive space-time tokenization for videos. *Advances in Neural Information Processing Systems*, 34, 2021.

C. Schuhmann, R. Vencu, R. Beaumont, R. Kaczmarczyk, C. Mullis, A. Katta, T. Coombes, J. Jitsev, and A. Komatsuzaki. Laion-400m: Open dataset of clip-filtered 400 million image-text pairs. *arXiv preprint arXiv:2111.02114*, 2021.

P. Sharma, N. Ding, S. Goodman, and R. Soricut. Conceptual captions: A cleaned, hypernymed, image alt-text dataset for automatic image captioning. In *Annual Meeting of the Association for Computational Linguistics (Volume 1: Long Papers)*, pages 2556–2565, 2018.

Y. Song, S. Shi, J. Li, and H. Zhang. Directional skip-gram: Explicitly distinguishing left and right context for word embeddings. In *Proceedings of the 2018 Conference of the North American Chapter of the Association for Computational Linguistics: Human Language Technologies, Volume 2 (Short Papers)*, pages 175–180, 2018.

K. Srinivasan, K. Raman, J. Chen, M. Bendersky, and M. Najork. Wit: Wikipedia-based image text dataset for multimodal multilingual machine learning. In *Proceedings of the 44th International ACM SIGIR Conference on Research and Development in Information Retrieval*, pages 2443–2449, 2021.

J. A. Stuart and J. D. Owens. Multi-gpu mapreduce on gpu clusters. In *2011 IEEE International Parallel & Distributed Processing Symposium*, pages 1068–1079. IEEE, 2011.

C. Sun, A. Shrivastava, S. Singh, and A. Gupta. Revisiting unreasonable effectiveness of data in deep learning era. In *Proceedings of the IEEE international conference on computer vision*, pages 843–852, 2017.

S. Sun, Y.-C. Chen, L. Li, S. Wang, Y. Fang, and J. Liu. Lightningdot: Pre-training visual-semantic embeddings for real-time image-text retrieval. In *Proceedings of the 2021 Conference of the North American Chapter of the Association for Computational Linguistics: Human Language Technologies*, pages 982–997, 2021.

B. Thomee, D. A. Shamma, G. Friedland, B. Elizalde, K. Ni, D. Poland, D. Borth, and L.-J. Li. Yfcc100m: The new data in multimedia research. *Communications of the ACM*, 59(2):64–73, 2016.

L. Wang, Y. Li, J. Huang, and S. Lazebnik. Learning two-branch neural networks for image-text matching tasks. *IEEE Transactions on Pattern Analysis and Machine Intelligence*, 41(2):394–407, 2018.

J. Wehrmann, D. M. Souza, M. A. Lopes, and R. C. Barros. Language-agnostic visual-semantic embeddings. In *Proceedings of the IEEE/CVF International Conference on Computer Vision*, pages 5804–5813, 2019.

J. Wu, H. Zheng, B. Zhao, Y. Li, B. Yan, R. Liang, W. Wang, S. Zhou, G. Lin, Y. Fu, et al. Ai challenger: A large-scale dataset for going deeper in image understanding. *arXiv preprint arXiv:1711.06475*, 2017.

Y. Wu, M. Schuster, Z. Chen, Q. V. Le, M. Norouzi, W. Macherey, M. Krikun, Y. Cao, Q. Gao, K. Macherey, J. Klingner, A. Shah, M. Johnson, X. Liu, L. Kaiser, S. Gouws, Y. Kato, T. Kudo, H. Kazawa, K. Stevens, G. Kurian, N. Patil, W. Wang, C. Young, J. Smith, J. Riesa, A. Rudnick, O. Vinyals, G. Corrado, M. Hughes, and J. Dean. Google’s neural machine translation system: Bridging the gap between human and machine translation. *arXiv preprint arXiv:1609.08144*, 2016.

L. Yao, R. Huang, L. Hou, G. Lu, M. Niu, H. Xu, X. Liang, Z. Li, X. Jiang, and C. Xu. Filip: Fine-grained interactive language-image pre-training. In *ICLR*, 2022.

Y. You, J. Li, S. Reddi, J. Hseu, S. Kumar, S. Bhojanapalli, X. Song, J. Demmel, K. Keutzer, and C.-J. Hsieh. Large batch optimization for deep learning: Training bert in 76 minutes. In *International Conference on Learning Representations*, 2020.

P. Young, A. Lai, M. Hodosh, and J. Hockenmaier. From image descriptions to visual denotations: New similarity metrics for semantic inference over event descriptions. *Transactions of the Association for Computational Linguistics*, 2:67–78, 2014.

X. Zhai, A. Kolesnikov, N. Houlsby, and L. Beyer. Scaling vision transformers. *arXiv preprint arXiv:2106.04560*, 2021a.

X. Zhai, X. Wang, B. Mustafa, A. Steiner, D. Keysers, A. Kolesnikov, and L. Beyer. Lit: Zero-shot transfer with locked-image text tuning. *arXiv preprint arXiv:2111.07991*, 2021b.

X. Zhan, Y. Wu, X. Dong, Y. Wei, M. Lu, Y. Zhang, H. Xu, and X. Liang. Product1m: Towards weakly supervised instance-level product retrieval via cross-modal pretraining. In *International Conference on Computer Vision*, 2021.

M. Zhou, L. Zhou, S. Wang, Y. Cheng, L. Li, Z. Yu, and J. Liu. Uc2: Universal cross-lingual cross-modal vision-and-language pre-training. In *Proceedings of the IEEE/CVF Conference on Computer Vision and Pattern Recognition*, pages 4155–4165, 2021.

A Appendix

A.1 Prompt Template

As previously observed in GPT-3 (Brown et al., 2020), the zero-shot performance can be significantly improved by customizing the prompt templates to each task. CLIP (Radford et al., 2021) also shows that specifying the category for each dataset contributes to the performance. However, since we only aim to provide a Chinese dataset with a general benchmarking of our released models, we leave the “prompt engineering” to the future work. We simply use the reported 80 general English prompts in CLIP and translate them to Chinese manually, as follows. Note that “{}” is replaced by the exact Chinese label name.

Chinese Prompts: “{}的照片。”，“许多{}的照片。”，“一张包含{}的照片。”，“质量差的{}的照片。”，“{}的雕塑。”，“难以看到{}的照片。”，“{}的低分辨率照片。”，“{}的渲染。”，“涂鸦{}。”，“{}的糟糕照片。”，“{}的裁剪照片。”，“{}的纹身。”，“{}的刺绣照片。”，“很难看到{}的照片。”，“{}的明亮照片。”，“一张干净的{}的照片。”，“{}的深色照片。”，“{}的手绘画。”，“我的{}的照片。”，“不自然的{}的照片。”，“一张酷的{}的照片。”，“{}的特写照片。”，“{}的黑白照片。”，“一幅{}的画。”，“一幅{}的绘画。”，“一张{}的像素照片。”，“{}的雕像。”，“一张{}的明亮照片。”，“{}的裁剪照片。”，“人造的{}的照片。”，“一张关于{}的照片。”，“损坏的{}的jpeg照片。”，“{}的模糊照片。”，“{}的相片。”，“一张{}的好照片。”，“{}的渲染照。”，“视频游戏中的{}。”，“一张{}的照片。”，“{}的涂鸦。”，“{}的近距离照片。”，“{}的折纸。”，“{}在视频游戏中。”，“{}的草图。”，“{}的涂鸦照。”，“{}的折纸形状。”，“低分辨率的{}的照片。”，“玩具{}。”，“{}的副本。”，“{}的干净的照片。”，“一张大{}的照片。”，“{}的重现。”，“一张漂亮的{}的照片。”，“一张奇怪的{}的照片。”，“模糊的{}的照片。”，“卡通{}。”，“{}的艺术作品。”，“{}的素描。”，“刺绣{}。”，“{}的像素照。”，“{}的拍照。”，“{}的损坏的照片。”，“高质量的{}的照片。”，“毛绒玩具{}。”，“漂亮的{}的照片。”，“小{}的照片。”，“照片是奇怪的{}。”，“漫画{}。”，“{}的艺术照。”，“{}的图形。”，“大{}的照片。”，“黑白的{}的照片。”，“{}毛绒玩具。”，“一张{}的深色照片。”，“{}的摄影图。”，“{}的涂鸦照。”，“玩具形状的{}。”，“拍了{}的照片。”，“酷酷的{}的照片。”，“照片里的小{}。”，“{}的刺青。”

A.2 Image-text retrieval dataset.

The data scale of datasets for image-text retrieval is described in Table 8. The texts in Flickr8K-CN, COCO-CN, AIC-ICC are human-annotated, the texts in Flickr30K-CN train/val set are machine-translated while the texts in Flickr30K-CN test set are human-translated from their original English counterparts. In Flickr8K-CN, Flickr30K-CN and AIC-ICC, each image is paired with 5 texts. In COCO-CN, each image is paired with 1 to 2 texts. In MUGE, each text is paired with 1 to 2 images in the train set, and with about 6 images in the val/test sets.

Table 8: Statistics of each image-text retrieval dataset.

Dataset	split	#Images	#Sentences
Flickr8K-CN (Li et al., 2016)	train	6,000	30,000
	val	1,000	5,000
	test	1,000	5,000
Flickr30K-CN (Lan et al., 2017)	train	29,783	148,915
	val	1,000	5,000
	test	1,000	5,000
COCO-CN (Li et al., 2019b)	train	18,341	20,065
	val	1,000	1,100
	test	1,000	1,053
AIC-ICC (Wu et al., 2017)	train	210,000	1,050,000
	val	30,000	150,000
	test-1	30,000	150,000
	test-2	30,000	150,000
MUGE (Lin et al., 2021)	train	129,380	248,786
	val	29,806	5,008
	test	30,399	5,004